Minoli, S., Egli, D. B., Rolinski, S., Müller, C. (2019): Modelling cropping periods of grain crops at the global scale. - Global and Planetary Change, 174, 35-46

DOI: 10.1016/j.gloplacha.2018.12.013

Title: Modelling cropping periods of grain crops at the global scale

Short title: Modelling global cropping periods

For submission to: Global and Planetary Change

Manuscript Type: Research paper

Names of all authors: Sara Minoli, Dennis B. Egli, Susanne Rolinski, Christoph Müller

Postal addresses and email addresses of the authors:

- Sara Minoli: Potsdam Institute for Climate Impact Research (PIK), Member of the Leibniz Association, Climate Impacts and Vulnerabilities, P.O. Box 60 12 03, D-14412 Potsdam, Germany, **sara.minoli@pik-potsdam.de**
- Dennis B. Egli: Department of Plant and Soil Sciences, University of Kentucky, Lexington, KY 40546-0312, **degli@uky.edu**
- Susanne Rolinski: Potsdam Institute for Climate Impact Research (PIK), Member of the Leibniz Association, Climate Impacts and Vulnerabilities, P.O. Box 60 12 03, D-14412 Potsdam, Germany, **rolinski@pik-potsdam.de**
- Christoph Müller: Potsdam Institute for Climate Impact Research (PIK), Member of the Leibniz Association, Climate Impacts and Vulnerabilities, P.O. Box 60 12 03, D-14412 Potsdam, Germany, **cmueller@pik-potsdam.de**

Name of corresponding author: Sara Minoli

Abstract

Crop models require information on both weather and agronomic decisions to simulate crop productivity and to design adaptation strategies. Due to the lack of observational data, previous studies used different approaches to determine sowing dates and cultivar parameters. However, the timing of harvest has not yet been sufficiently analyzed.

Here we propose an algorithm to determine location-specific maturity (or harvest) dates for applications in global modelling studies. Given a sowing date and the climatic conditions, the algorithm returns a suitable maturity date, based on crop physiological parameters and agronomic principles.

We test the method on a global land area with a spatial resolution of 0.5° against global reported datasets for major grain crops*:* winter-wheat, spring-wheat, rice, maize, sorghum and soybean. A single set of rules is able to largely reproduce the observed harvest dates of the six grain crops globally, with a mean absolute error of 19 (maize) to 45 (rice) days. In temperate regions, the temperature seasonality is the major driver of cropping calendars. In sub-tropical regions, crops are grown to match water availability. In the case of limiting growing seasons, the crop cycle is shortened or extended to avoid stressful periods. In the case of long-lasting favorable conditions the crop cycle is shorter than what the growing season would allow.

We find that cropping periods can be largely defined by climate and crop physiological traits. The timing of the reproductive phase is shown to be a general criterion for selecting grain crops cultivars. This work will allow for dynamically representing adaptation to climate change by adjusting cultivars and represents a first step towards improved crop phenology simulations by global-scale crop models.

Keywords

cropping calendar; maturity date; growing period; cultivar; phenology; temperature threshold; agricultural management; modelling.

1. Introduction

According to the fifth IPCC Assessment Report (IPCC, 2013) over the 21st century global mean temperatures will continue to rise, with stronger trends over land, and future precipitation changes will result in exacerbated patterns of wet and dry regions. Changes in climatic factors affect crop growth and therefore the productivity of agricultural systems, posing challenges to the sustenance of human societies (Asseng et al., 2015). Realistic representation of agricultural systems is a major concern in the context of global change studies (Makowsky et al., 2014). Agronomic practices, including crop management, characterize agroecosystems and are crucial in defining adaptation strategies (Ainsworth & Ort, 2010; Tomic et al., 2011; Porter et al., 2014). The choice of crop cultivar is the foremost management option to optimize crop productivity, and to adapt to climate change (e.g. Singh et al., 2013; Macholdt & Honermeier, 2016; Challinor et al., 2016). Crop cultivars are bred for different traits, such as phenology, habit, productivity, vigor, resistance to pathogens, seed quality, etc. Out of these, phenological traits are prioritized in most cases, because of the importance in matching the plant cycle to growing season conditions, such as temperature or water supply (Sedgley, 1991; Craufurd & Wheeler, 2009).

Crop phenological development constitutes a relevant source of crop model uncertainties (Koehler et al., 2013; Jägermeyr & Frieler, 2018). Models typically simulate the crop phenology based on the thermal time concept (Ritchie & NeSmith, 1991; Wang et al., 2017). Starting from the sowing (or planting) date growing-degree-days are accumulated until thermal unit requirements are met, corresponding to crop maturity (or harvest) date (e.g. Kucharik & Brye, 2003). Reduction factors can be included to eventually simulate the sensitivity to photoperiod and vernalization of some crops. Thermal unit requirements are therefore key parameters of the majority of crop models, that are used to represent the cultivar diversity and that are typically the first to be calibrated for matching the crop cycle duration (Archontoulis et al., 2014).

Due to a lack of information, different approaches have been developed to represent cultivar diversity distribution in global-scale models. Before the first global datasets on sowing and harvest dates were published (Portmann et al., 2010; Sacks et al., 2010), Bondeau et al. (2007) modelled crop-specific sowing dates as a function of climate and the thermal unit requirements as directly dependent on the sowing date, so that e.g. crops sown in warmer climates would require more growing-degree-days to complete their cycle. Similarly, Lindeskog et al. (2013) used a 10-years running mean of thermal unit requirements between default sowing and harvest date limits.

Global datasets can be used to prescribe sowing dates and to directly calibrate crop models in order to match observed harvest dates (Deryng et al., 2011; Drewniak et al., 2013; Elliott et al., 2015). Such approach is possible if observations are available, which limits it applicability to only those areas where the crop is currently grown and observational data sets are of sufficiently good quality. Moreover, if applied under e.g. future climate scenarios, it does not allow for accounting for eventual adjustments in cultivars selection so that assessments of climate change impacts on agricultural productivity often assume static cultivar selection (Rosenzweig et al. 2014).

To overcome this, van Bussel et al. (2015) derived algorithms to compute location-specific phenological parameters (thermal unit requirements and photoperiod factors) from climatic variables. The algorithm, tested on wheat and maize only, can be applied also outside the current cropland as well as under climate change. One limitation is that it requires a model that uses the specific response functions to temperature and photoperiod applied by the authors. However, crop models can be very diverse in the mathematical functions they use, which themselves constitute a large source of model diversity and of uncertainty (Wang et al., 2017).

Another approach is to estimate sowing and harvest dates, and to use these for model phenology parametrization, similarly to prescribing observed datasets (Mathison et al., 2018). Sacks et al. (2010) found that sowing dates of wheat and maize are dependent on temperature, and can be predicted by fixed temperature thresholds, especially in temperate regions. Waha et al. (2012) simulated sowing dates of several crops at the global scale, taking into account both temperature and precipitation. Other approaches were proposed for regional applications, to estimate sowing dates based on soil temperature and soil moisture (Dobor et al., 2016) or both sowing and harvest dates based on the monsoon onset and retreat; (Mathison et al., 2018).

In this paper we develop an algorithm to determine location-specific cropping periods for applications in global modelling studies so that adaptation in growing periods under climate change can be explicitly addressed. The approach can be used in combination with either prescribed or computed sowing dates. Given a sowing date, the algorithm returns a suitable maturity (or harvest) date, based on a) crop physiological parameters; b) climatic conditions; c) agronomic principles for maximizing crop productivity. We test the method on a global land area with a spatial resolution of 0.5° against global reported datasets.

2. Methods

2.1. Overview

The purpose of the model is to estimate location-specific average maturity dates of grain crops. The model has been designed particularly for applications in global scale studies, to allow for calibrating long-term average phenology (e.g. thermal unit requirements) in crop models, in order to represent geographical patterns of crop cultivar diversity and their adaptation.

Only major *grain crops* were included in this study, in particular winter-wheat (*Triticum* sp. L.), spring-wheat (*Triticum* sp. L.), rice (*Oryza sativa* L.), maize (*Zea mays* L.), sorghum (*Sorghum bicolor* L. Moench), and soybean (*Glycine max* L. Merr.). These crops have dry seeds (grains) as the harvestable product. Moreover, only rainfed cultivation systems were considered.

The model unit consists of two entities: a human-agent (individual farmer) and a grain crop species, and two location-specific exogenous drivers: the climate and the average crop sowing date. Farmers are characterized by their location (grid cell) and their knowledge about the best growing conditions for each crop. Crops are characterized by a set of parameters, which are the agronomic potential duration of their crop cycle (sowing to maturity) and the repartition of this cycle into a vegetative and a reproductive phase. The latter phase is, in turn, characterized by thresholds of base and optimum temperatures and of two different soil moisture indicators. The model is run on a global-land grid at 0.5° x 0.5° spatial resolution and returns for each grid cell a long-term average daily maturity date (state variable).

In a given year, the farmer grows a given crop in a given location and makes a decision on the best sowing date and on which cultivar to grow. The model we present here focuses on the cultivar choice. Models for computing both average and yearly sowing dates are already available, therefore we use sowing dates as exogenous variables. Each farmer considers the experienced climate and seasonality of the previous 20 years, as well as crop-specific environmental limits to identify the most suitable growing period (sowing-to-maturity time) for the considered grain crop.

The modelling workflow (Figure 1a) includes 1) the review of literature on crop physiological parameters, from which we derived crop temperature parameters; 2) the analysis of climate data and of observed crop calendars, from which we estimated the water availability parameters; 3) the development and parametrization of the rules to estimate the maturity date; 4) the evaluation of the rule against observed crop calendars; 5) the re-calibration of the parameters within the predefined range. Figure 1b shows the decision tree for the agronomic rules to compute maturity dates (grey box in Figure 1a).

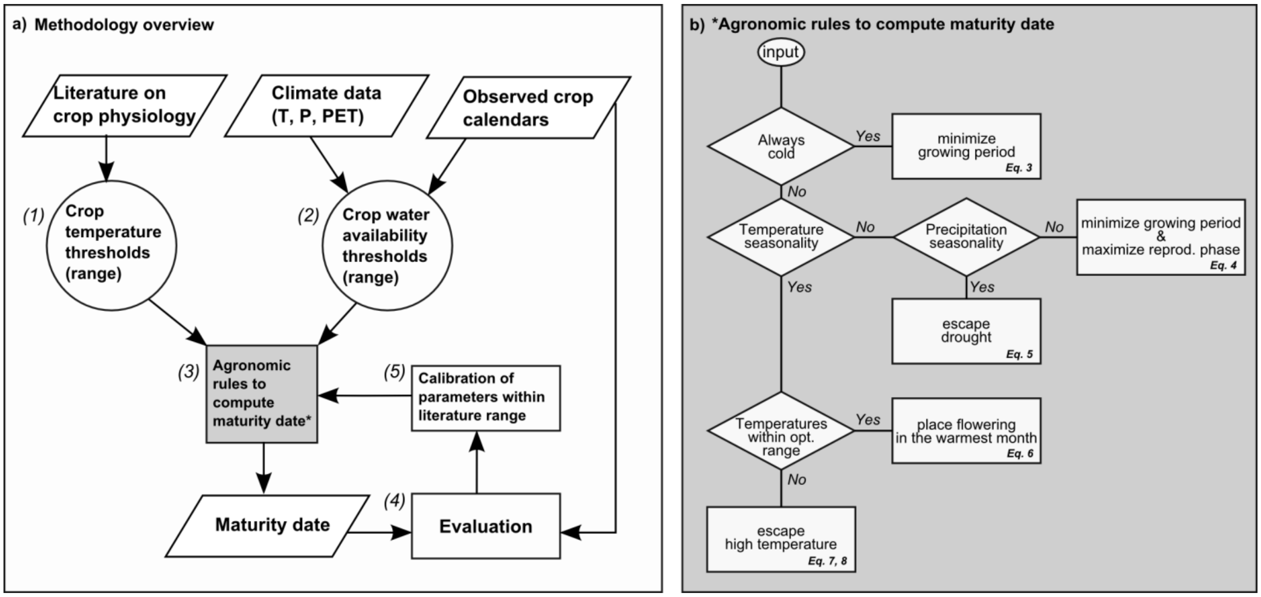

Figure 1. Representation of the modelling workflow (a) and details of the agronomic rules to compute the maturity dates (b). In (a) the parallelograms represent inputs or outputs, circles represent parameters, rectangles represent processes. In the decision tree (b) diamonds represent decision and rectangles depict the maturity date rules.

2.2. Model design concepts

Phenological development largely determines the suitability of a crop for a certain range of environmental conditions (Slafer et al., 2015). We distinguish between "*growing seasons*" and "*growing periods*". The growing season is the period of time in the year during which environmental conditions are suitable for a given crop to growth, while the crop growing period is the period of time from sowing to maturity (Waha et al., 2013). Therefore, the growing season might be longer than the growing period, as in some cases there is no advantage of growing a crop longer than needed for maximizing yield.

We review agronomical principles for adapting crop phenology to local climate. We formalize these principles by 1) choosing a representation of the phenological cycle common to all grain crops; 2) deriving crop-specific environmental limits from literature; 3) defining a classification of agro-climatic zones; 4) defining rules to identify the most suitable cropping period for the considered grain crops in each location (grid cell). A cropping period is identified as "most suitable" when the reproductive growth phase is maximized while the risk of encountering stressful environmental conditions is minimized.

2.2.1. Agronomic principles for identifying the most suitable cropping period

To be suitable, a grain crop must flower sufficiently early for seeds to mature while favorable conditions persist. However, if flowering is too precocious, plant growth may be insufficient to sustain seed yield (Lawn et al., 1995). The crop biomass production is indeed a cumulative process that requires time to first capture solar radiation to convert its energy into photosynthetic assimilates, and then to build the reproductive and the storage organs from these. The total biomass can be maximized by letting the crop use as much solar radiation as possible, by matching the length of the phenological development to the length of the growing season (Egli, 2011). In the case of short growing seasons, this way also highest grain yields are gained as often occurs at high latitudes (Peltonen-Sainio et al., 2015) or altitudes, or in very dry environments (Bodner et al., 2015). On the contrary, in the case of long and favorable seasons, a crop cycle shorter than the growing season may be sufficient to obtain the maximum grain yield. In particular, this is valid when the total growth length exceeds the duration where reproductive growth, and therefore yield, stops increasing (Egli, 2011). However, long growing seasons might also include or terminate with stressful periods. Under these conditions, the use of late- or early-maturing cultivars may be strategic for shifting the reproductive growth to a more favorable period, to avoid stresses and yield losses (Craufurd & Qi, 2001; Clerget et al., 2008; Egli, 2011).

For an effective crop establishment, sowing should be carried out when soil temperature allows for rapid seed germination and seedlings emergence (Waha et al., 2012). Grain yield can be maximized when the crop is exposed to an optimum range of air temperature, and it progressively declines as temperature increases above this range (Hatfield et al., 2011). Grain crops are generally more sensitive to high temperatures during the reproductive than the vegetative development stages (Farooq et al., 2011; Singh et al., 2013).

To enable yield formation, soil water content must be sufficient to sustain crop growth throughout the entire growing period. Ensuring an adequate water supply during grain filling is particularly critical for grain yield in annual crops (Asseng et al., 2015). Therefore, in regions strongly characterized by precipitation seasonality, the growing season is dependent on the onset and cessation of the rain (Araya et al., 2010; Bodner et al., 2015; Mathison et al., 2018).

2.2.2. Definition of the crop phenological cycle and environmental limits

The duration of the total growing period (GP) can vary widely among locations, crops and cultivars. We set lower (GPmin) and upper (GPmax) limits as indications of the biological (or agronomical) potential of the crops. We consider the *vegetative phase* (GPV) to have a flexible duration, while we assume the *reproductive phase* (GPR) to have a constant length equivalent to its maximum if the growing period is long enough to support this (Table 1). The time allocated to vegetative and reproductive growth follows a similar pattern in all grain crops. According to Egli (2011), the actual yield formation period (reproductive phase) becomes nearly constant after approaching a maximum (horizontal asymptote). Conversely, the vegetative phase increases steadily with the total growth length. All crop species share the same relationship, except maize, which allocates a longer time to the reproductive phase. We call GPmaxrp the minimum growing period for attaining the longest reproductive phase. For all growing periods that are shorter than GPmaxrp, the GPR is shorter than the parameter specified in Table 1. However, as the model does not simulate anthesis dates, the length of the actual GPR is not explicitly computed.

In this work we represent the crop cycle by just two main phases, namely the vegetative and the reproductive phase. There are a number of metrics to describe the phenological development of the grain crops (e.g. BBCH (Meier, 1997), Vn-Rn stages, etc.). In several crops, these two periods overlap, so that they can be arbitrarily defined depending on the scope of the work. Here we call *vegetative* (GPV) the phase from sowing, or more precisely from germination (BBCH 09), to the end of flowering (BBCH 69), while we call *reproductive* (GPR) the phase lasting from the beginning of the grain development (BBCH 70) to the grain physiological maturity (BBCH 89). Additionally, we take into account the *senescence* phase (MatHar) from physiological maturity to the stage of harvestable grain (BBCH 99) (Table 1).

We use cardinal *base temperatures for reproductive development* (T_{baseRD}) and *optimum temperatures for reproductive production* (T_{optRP}) (Hatfield et al., 2011), as thresholds to identify the best time for the crop reproductive phase, and consequently for the end of the growing period of a crop in a given location (Table 2). Together with temperature, the crop cycle is largely influenced by water availability. We use water availability thresholds of $PPET_{ratio}$ and $PPET_{ratioDIFF}$ (Table 2) to identify the last convenient period for crop growth.

2.2.3. Rule-based decision making

We assume one farmer agent for each grid cell, and that all farmers have the same knowledge and crop cultivar availability. The decision making on the most suitable average maturity date for a certain crop and location is modelled by a set of rules (see below for the details). In a given year, the farmer takes into account the long-term average temperature and precipitation seasonality of the previous 20 years in that location and the environmental limits to the crop reproductive growth to define the growing period that maximizes the reproductive growth duration, while minimizing the risk of encountering stressful environmental conditions. We assume that the farmer does not rely on any information about pre-season weather forecasts, but that he/she expects the weather of the year-of-simulation to be close to the previous 20 years average.

Table 1: Crop-specific parameters (growth phase lengths) of the maturity date function. Phases are defined by the BBCH scale (Meier, 1997). The total growing period (GP) is defined as the sum of vegetative (GPV) and reproductive (GPR) growing periods. GPmin and GPmax are the minimum and the maximum allowed GP, respectively. GPmaxrp is the minimum growing period for attaining the longest reproductive phase. The parameter GPR denotes the maximum length of the reproductive growing period for growing periods longer than GPmaxrp.

growth phase	vegetative	reproductive	limits of GP			maturity to harvest
BBCH	(00-69)	(70-89)	(00-89)			(89-99)
parameter	GPV	GPR	GPmin	GPmax	GPmaxrp	MatHar
unit	(days)	(days)	(days)	(days)	(days)	(days)
winter-wheat	internal[1]	40[2]	60[2]	330[3]	120[2]	7[4]
spring-wheat	internal[1]	40[2]	60[2]	180[2]	120[2]	7[4]
rice	internal[1]	40[2]	60[2]	180[2]	120[2]	7[4]
maize	internal[1]	60[2]	60[2]	180[2]	120[2]	21[4]
sorghum	internal[1]	40[2]	60[2]	180[2]	120[2]	0[4]
soybean	internal[1]	40[2]	60[2]	180[2]	120[2]	21[4]

(1) internally computed in the model

(2) Egli (2011)

(3) Rukhovich et al. (2007)

(4) Elliott et al. (2015)

Table 2: Crop-specific parameters (temperature (°C) and water thresholds (dimensionless)) used in the maturity date function and their reference values from literature. TbaseRD is the base temperature for reproductive development, ToptRP is the optimum temperature for reproductive production (grain-filling), PPETratio is the ratio between precipitation and evapotranspiration in a month, PPETratioDIFF is the monthly trend in moisture conditions. Mean and ranges of parameter values found in literature are from five review studies (Porter & Gawith, 1999; Hatfield et al., 2011; Farooq et al., 2011; Singh et al., 2013; Sánchez et al., 2014). Temperature thresholds for sowing can be found in Waha et al. (2012).

Parameter Unit	T_{baseRD} (°C)				T_{optRP} (°C)				$PPET_{ratio}$ (-)	$PPET_{ratioDIFF}$ (-)
	values found in literature			values used in this study(1)	values found in literature			values used in this study(2)	values used in this study(3)	values used in this study(3)
Crop	mean	range	ref.		mean	range	ref.			
winter-wheat	9.5	(9 - 12)	a	1	20.7	(15 - 25)	a	21 (12 - 25)	NA	NA
	1		b		15	(15 - 25)	b			
					21.3	(12 - 22)	c			
spring-wheat	9.5	(9 - 12)	a	1	20.7	(15 - 25)	a	25 (12 - 25)	0.5 (0 - 1)	0.5 (0.1-0.5)
	1		b		15	(15 - 25)	b			
					21.3	(12 - 22)	c			
rice	8		b	8	25	(23 - 26)	b	24 (20 - 31)	1.0 (0 - 1)	0.5 (0.1-0.5)
	20.7	(12 - 14)	d		24.2	(20 - 31)	d			
maize	8		b	7	24	(18 - 30)	b	30 (18 - 30)	0.5 (0 - 1)	0.5 (0.1-0.5)
	8	(7 - 16)	d		< 30		e			
					26.4	(25 - 30)	d			
sorghum	8		b	8	25	(25 - 28)	b	25 (25 - 28)	0.5 (0 - 1)	0.5 (0.1-0.5)
soybean	6		b	6	23	(22 - 24)	b	23 (22 - 27)	0.5 (0 - 1)	0.5 (0.1-0.5)
					23	(23 - 27)	e			

(1) values of TbaseRD used in this study were selected as the minimum of the overall range reported in the references.
(2) values of ToptRP used in this study based on the sensitivity analysis. In brackets the overall range reported in the references. The selected value was chosen as the one that can best reproduce the observed cropping calendars (minimum MAE).
(3) values of PPETratio and PPETratioDIFF used in this study based on the sensitivity analysis. In brackets the tested range. The selected value was chosen as the one that can best reproduce the observed cropping calendars (minimum MAE).
(a) Porter & Gawith, 1999
(b) Hatfield et al., 2011
(c) Farooq et al., 2011
(d) Sánchez et al., 2014
(e) Singh et al., 2013

2.3. Model details

2.3.1. Climate data and statistics

In this model application, we simulate maturity dates for the year 2000. As we assume farmers to make decisions on the preceding 20 years, we computed monthly statistics for the period 1980-1999. Data of the following climatic variables were derived from the AgMERRA global climate forcing dataset with daily time steps (Ruane et al., 2015), that we use at 0.5° x 0.5° spatial resolution (Elliott et al., 2015). We computed the monthly mean temperature (T, °C) as the average of the daily mean temperature of all days of each month: the monthly cumulated precipitation (P, mm month^{-1}) as the sum of the daily precipitation in that month; the monthly cumulated potential evapotranspiration (PET, mm month^{-1}) as the sum of the daily PET rate in that month, estimated with the Priestley-Taylor equation (Priestley & Taylor, 1972), with a Priestley-Taylor coefficient of 1.391 (Gerten et al., 2004). Additionally we computed two monthly dryness indices based on P and PET. The simple P to PET ratio ($PPET_{ratio}$, dimensionless, Eq. 1) indicates the water surplus or deficit with respect to the plants water demand (Thornthwaite, 1948; Sacks et al., 2010; van Wart et al., 2013), and the $PPET_{ratio}$ difference of two consecutive months ($PPET_{ratioDIFF}$, dimensionless, Eq. 2) indicates the monthly trend in moisture conditions. If $PPET_{ratioDIFFm}>0$, the trend is declining, indicating that the following month (m+1) is dryer than month m.

$$PPET_{ratio_m} = P_m / PET_m \qquad \text{(Eq. 1)}$$

$$PPET_{ratioDIFF_m} = PPET_{ratio_m} - PPET_{ratio_{m+1}} \qquad \text{(Eq. 2)}$$

Long-term daily averages are obtained by linear interpolation of the monthly statistics, to cope with fluctuations of daily values, and to allow for the consideration of monthly input data.

2.3.2. Agro-climatic zones classification

Agro-climatic zones can be defined based on homogeneity in the weather variables that have greatest influence on crop growth and yield (van Wart et al., 2013), such as temperature and water availability. According to Waha et al. (2012) we define three climate zones (seasonality types) by the intra-annual variability (coefficient of variation, CV) of T (CV_{temp}) and P (CV_{prec}). These are computed on monthly climate data:

1) no temperature and no precipitation seasonality (NO SEAS.: CV_{prec} ≤0.4 AND CV_{temp} ≤0.01);

2) precipitation seasonality (PREC. SEAS.: CV_{prec} >0.4 AND CV_{temp} ≤0.01);

3) mixed seasonality (MIXED SEAS.: CV_{temp} >0.01 AND (CV_{prec} ≤0.4 OR CV_{prec} >0.4)).

In addition to that, we consider the temperature of the warmest month (max(T)) and compare it to the crop-specific thresholds for reproductive growth (T_{baseRD}, T_{optRP}). Within each seasonality type, three possible temperature configurations can occur:

(a) temperatures never reach the base temperature ($max(T)<T_{baseRD}$), so that the crop cannot complete its reproductive cycle, and therefore cannot productively be grown;

(b) temperatures exceed T_{baseRD}, while never exceeding the optimum temperature T_{optRP}, so that at least part of the year is available for the crop to go through its reproductive cycle;

(c) temperatures exceed T_{optRP}, so that at least part of the year is characterized by supra-optimal temperatures for yield production (see Appendix A).

2.3.3. Function to compute the maturity date

The set of rules for estimating the end of the growing period (date of physiological maturity) is graphically described in Figure 1b and in Appendix A and all parameters are listed in Table 1 and Table 2. The seasonality type determines which climatic factor (temperature or precipitation, or their combination), is the most limiting for the total crop cycle. Differences between the monthly mean temperature (T) level and T_{baseRD} and T_{optRP} define the existence of a suitable period for the reproductive growth. In the following formulas, rule numbers 1, 2, 3 refer to the seasonality types NO SEAS., PREC. SEAS, MIXED SEAS., and letters a, b, c, refer to the temperature levels LOW T., MID T., HIGH T. respectively. Moreover, Sowing day is the day of the year on which the growing period starts and it can be either prescribed or simulated by any algorithm (e.g. Waha et al., 2012), T_{max} day is the day on which the warmest temperature is reached (here assumed to be the midday of the warmest month); T_{opt} day1 is the first day on which T > T_{optRP}, T_{opt} day2 is the last day of T > T_{optRP}. $PPET_{ratio}$ day is the first day on which the $PPET_{ratio}$ or $PPET_{ratioDIFF}$ falls below the defined threshold (Table 2). The rule for simulating the maturity date is defined as follows (see also Appendix A):

In regions characterized by very low temperatures, always below the base temperature for reproductive development (max(T) < T_{baseRD}), the shortest maturing cultivar is chosen, regardless of the seasonality type. The growing period is set to GP_{min} (agro-climatic zones 1.a, 2.a, 3.a; Eq. 3). This is a rule to ensure functionality at the global scale, and to allow the simulation in those environments where crops in fact cannot be grown.

$$Maturity\ day = Sowing\ day + GP_{min} \qquad \text{(Eq. 3)}$$

In warmer regions (max(T) > T_{baseRD}) without temperature seasonality, the crop can complete the reproductive cycle. We do not account for possible limitations due to too high temperature (failure temperature). If there is also no precipitation seasonality (NO SEAS. in Appendix A), the growing period is set equal to GP_{maxrp} (agro-climatic zones 1.b, 1.c; Eq. 4).

$$Maturity\ day = Sowing\ day + GP_{maxrp} \qquad \text{(Eq. 4)}$$

Otherwise, under precipitation seasonality (PREC. SEAS. in Appendix A), the maturity date might be anticipated to escape drought. The reproductive phase (GPR) is set to start towards the end of the wet-season ($PPET_{ratio}$ day), to guarantee soil water availability until maturity (agro-climatic zones 2.b, 2.c; Eq. 5).

$$Maturity\ day = \min \begin{cases} PPET_{ratio} day + GPR \\ Sowing\ day + GP_{maxrp} \end{cases} \quad \text{(Eq. 5)}$$

In regions with temperature and eventually precipitation seasonality (MIXED SEAS. in Appendix A), the maturity date is determined by setting the reproductive phase in the most suitable period of the year, to minimize stresses, and to leave sufficient time to develop photosynthetic organs. The most limiting factor is the one that occurs first. The growing period cannot be shorter or longer than GP_{min} or GP_{max} respectively.

Under mid temperature conditions (T_{optRP} > max(T) > T_{baseRD}), the reproductive phase starts at the warmest day of the year (T_{max} day) (agro-climatic zone 3.b; Eq. 6).

$$Maturity\ day = \min \begin{cases} \max(Sowing\ day + GP_{min};\ T_{max} day + GPR) \\ \max(Sowing\ day + GP_{min};\ PPET_{ratio} day + GPR) \\ Sowing\ day + GP_{max} \end{cases} \quad \text{(Eq. 6)}$$

Under high temperature conditions (max(T) > T_{optRP}) (agro-climatic zone 3.c) we distinguish between winter and spring crop types:

Winter crops have a long time available for their vegetative growth that they can exploit during both autumn and spring. Maturity occurs as soon as the temperature exceeds the optimum temperature (T_{opt} day_1), so that the crop can escape high temperature stress by maturing beforehand. We assume no water limitations (Eq. 7).

$$Maturity\ day = \min \begin{cases} \max\left(Sowing\ day + GP_{min};\ T_{opt} day_1\right) \\ Sowing\ day + GP_{max} \end{cases} \quad \text{(Eq. 7)}$$

Spring crops need to use the first part of the season for developing photosynthetic organs, so that the earliest period of the season with optimal conditions for reproductive growth is in fact used for the vegetative phase. The start of the reproductive cycle is set when the mean temperature falls below the optimum temperature (T_{opt} day_2), to avoid the risks of high-temperature stress in the middle of the growing period, and to ensure the best conditions for the reproductive phase (Eq. 8).

$$Maturity\ day = \min \begin{cases} \max\left(Sowing\ day + GP_{min};\ T_{opt}day_2\right) \\ \max(Sowing\ day + GP_{min};\ PPET_{ratio}day) \\ Sowing\ day + GP_{max} \end{cases} \quad \text{(Eq. 8)}$$

For comparison with observational datasets, which report harvest dates rather than maturity dates, we estimate harvest dates by adding a crop-specific maturity to harvest (MatHar) time (Table 1) to the computed maturity dates (Eq. 9).

$$Harvest\ day = Maturity\ day + MatHar \quad \text{(Eq. 9)}$$

In summary, the end of the cropping period can be triggered by one of the following reasons: the choice of the earliest-maturing cultivar (GP_{min}); the cultivar with the longest grain-filling phase (GP_{maxrp}); the latest-maturing cultivar (GP_{max}); or the occurrence of water limitations (w. lim.); mid-temperature limitations (mid. t.); high-temperature limitations (high t.).

2.3.4. Model setup

We used R (R Core Team, 2015) for the model implementation, the data preparation, and the overall analysis. In order to examine its performance and sensitivity, we run the model with different parametrization settings and input data (Table 3).

Table 3: Summary table of model runs

Run setup ID	Number of runs per crop	Parametrization	Sowing date
1	315	sensitivity	MIRCA2000
2	1	calibrated	MIRCA2000
3	1	calibrated	SAGE
4	1	calibrated	Simulated (Waha et al., 2012)

2.3.5. Parametrization

For simplicity, we assume unique values of the model parameters to be valid globally. We derived parameters related to the growth phase lengths (GPR, GP_{min}, GP_{maxrp}, GP_{max}, MatHar) (Table 1) and to temperature thresholds (T_{baseRD}, T_{optRP}) from literature (Table 2). We were not able to find reference values of $PPET_{ratio}$ and $PPET_{ratioDIFF}$ thresholds or any other moisture-related thresholds for any specific growth phase. We therefore explored the patterns of the two variables throughout the observed growing periods (MIRCA2000). We find that except for winter- and spring-wheat, for all other crops $PPET_{ratio}$ starts declining from about two months before harvest, with the stronger negative trend ($PPET_{ratioDIFF}$) about one month before harvest (Appendix C).

2.3.6. Sensitivity analysis and calibration

We perform a sensitivity analysis of the maturity date function to T_{optRP}, $PPET_{ratio}$ and $PPET_{ratioDIFF}$ thresholds. For this we used MIRCA2000 sowing dates as the model input data. As the representativeness of the reported T_{optRP} range is not clear for each grain crop considered here, we also test whether the model behavior is substantially different outside the reported temperature range. Therefore, we run the model with different temperature thresholds ranging from 2°C below the lowest reported temperature threshold to 2°C above the reported temperature threshold in increments of one degree. For the moisture related thresholds we used ranges of representative values (0, 0.5, 1 for $PPET_{ratio}$ and 0.1, 0.2, 0.3, 0.4, 0.5 for $PPET_{ratioDIFF}$). Subsequently, we calibrate the function to MIRCA2000 by testing which thresholds can best reproduce the reported cropping calendars. We select the parameter set for each crop that leads to the lowest global area-weighted Mean Absolute Error (MAE) (see 2.4).

2.3.7. Model response to input data

We also compute cropping calendars by combining the calibrated maturity date function presented above with three different sowing date inputs: MIRCA2000, SAGE and simulated with sowing date function proposed by Waha et al. (2012).

2.4. Model evaluation

To evaluate the model's skill in estimating maturity dates, we compare global-scale simulations for the six crops for the year 2000 to the two most applied global cropping calendar datasets (MIRCA2000, Portmann et al. 2010, and SAGE, Sacks et al. 2010) in the modelling community. In order to exclude the uncertainty due to the sowing date, we prescribe the sowing date from the observation-based dataset.

The MIRCA2000 (v1.1) dataset (Portmann et al., 2010) provides monthly cropping periods of 26 crop types, as well as the associated growing areas, available at 0.5° grid cell resolution, representative for the time period 1998 to 2002. For our analysis, we refer to the rainfed sub-crops with the largest reported area for rice, maize, sorghum, soybeans. For wheat, we merged sub-crops 1 and 2 and distinguished between winter- and spring-wheat as follows (map shown in Appendix B). We assume that the growing season refers to winter-crop if (i) the cropping period includes the coldest month of the year, and (ii) the mean temperature of the coldest month is lower than 10°C.

The SAGE dataset (Sacks et al., 2010) provides typical planting and harvesting dates for 19 crops, available at 0.5° resolution, representative for the time for the 1990s or early 2000s. In comparison with MIRCA2000 this dataset (i) has a daily resolution; (ii) distinguishes between winter- and spring-wheat;

(iii) does not distinguish irrigated and rainfed crops; (iv) does not include data on crop area; (v) is often uniform in large administrative units such as countries.

For the evaluation of the goodness-of-fit of the model to the observed datasets, we employ the Mean Absolute Error (MAE) index (Jachner et al., 2007), area-weighted as in Waha et al. (2012).

$$MAE = \frac{\sum_{i=1}^{n} |S_i - O_i| \times A_i}{\sum_{i=1}^{n} A_i} \qquad \text{(Eq. 10)}$$

Where *n* is the number of observations (grid-cells with a reported harvest date), *i* is the index of the grid cell, *S* and *O* are respectively the simulated and observed date (months) of grid-cell *i*, A is the cropped area (ha) of grid-cell *i*. For weights, we use the crop area of MIRCA2000, which we also employ for masking uncropped areas in maps when displaying results.

3. Results

3.1. Model sensitivity and parametrization

The results of the model calibration reveal (Appendix D) that, with the exception of sorghum, temperature thresholds outside the reported ranges (Table 2) would not lead to better model performances. For sorghum, the minimum MAE is obtained with a T_{optRP} value of 1°C lower than the reported temperature range, but it is only marginally better than the lowest reported threshold temperature. Rice, soybean and winter-wheat show a U-shaped curve, with a minimum MAE in the middle of the tested temperature range, whereas maize and spring-wheat show best performances at the upper limit of the reported temperature range, but with stable MAE values above this.

The sensitivity to $PPET_{ratio}$ and $PPET_{ratioDIFF}$ indicate that most crops, except rice, perform best (minimum MAE) when both parameters are set to 0.5. This indicates that last phases of the crop growth cycles are shorter if there is either a period characterized by low P and/or high PET, or by a drastic change in the precipitation regime from wet to dry. The performance of the model for winter-wheat is completely insensitive to $PPET_{ratio}$ and $PPET_{ratioDIFF}$, as we assume no water limitation in the maturity date rule of this crop (Table 2).

3.2. Computed maturity dates

3.2.1. Aggregated model performances

At the global aggregation level, the calibrated model can largely reproduce the observed harvest months from both MIRCA2000 (calibration dataset) and SAGE (independent dataset), with an absolute error lower than 30 days for all crops except for rice (Figure 2). Specifically, for winter-wheat, spring-wheat, rice, maize, sorghum, and soybean, 82, 78, 61, 93, 82, 91% of the total area respectively, show an error within +/-1 month. The comparison against SAGE results in similar MAE values (Appendix E) and 90, 77, 54, 79, 58, 92% with an error within +/-1 month. The different criteria for determining the end of the cropping period are distributed across different error classes, so that no systematic error can be detected in any of the rules (Figure 2). High temperature limitations typically do not constrain growing periods of spring-wheat and maize. All crops are mostly grown for periods longer than their lower potential limit (GP_{min}), and shorter than their upper-potential (GP_{max}).

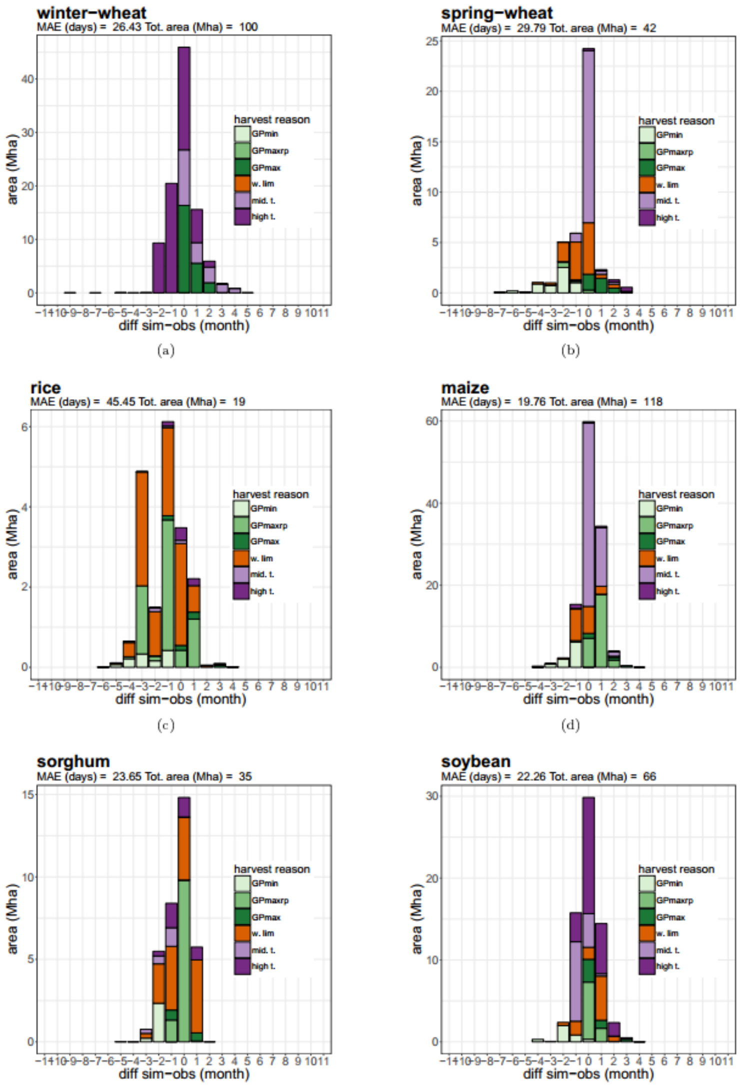

Figure 2: Aggregated performances of the model. Frequency distribution of the difference between simulated and observed (MIRCA2000) harvest dates. Frequency is measured in terms of harvested area (Mha). The colors indicate the reason that triggers the harvest. GP_{min} is earliest-maturing cultivar; GP_{maxrp} is longest grain-fill cultivar; GP_{max} is latest-maturing cultivar; w.lim is water limitations; mid. t. is mid-temperature limitations; hight t. is high-temperature limitations.

3.2.2. Global patterns

In this and the following sections of the main text we show results for maize only (Figure 3), as this crop has the largest cultivated area (Figure 2) and diversity of climates (Figure 3(a)). Results of all simulated crops are presented in Appendix F, but also discussed in the main text. We concentrate in the main text on the results of the simulation with prescribed sowing dates from MIRCA2000 (Figure 3) and provide a comparison of results with computed sowing dates (Waha et al., 2012) in Appendix G.

Maize is cultivated in nearly all considered climatic zones (Figure 3(a)) and therefore rules (Appendix A) for computing the maturity date are very diverse. Maize growing seasons encounter mean temperatures above the optimum (29°C) in sub-Saharan Africa and in India. The remaining maize cultivated area is characterized by average monthly temperature between T_{baseRD} and T_{optRP} for at least part of the year (Appendix E and F).

Various factors cause the end of maize growing period across regions (Figure 3(b)). In temperate regions the maize cycle follows the seasonal evolution of temperature (purple color, Figure 3(b)), resulting in fairly long (up to 7 months) total GPs (Figure 3(d)). In some areas, such as around the Mediterranean Sea, sub-Saharan and East Africa, South-East Asia (orange color, Figure 3(b)), the maturity date is triggered by the occurrence of a dry period (3 to 4 months GP). In parts of India and Mexico, either temperature or water limitation occur soon after sowing, determining a very short total GP (2 months). Within the tropics large areas show no constraints for maize to grow for up to 5 months.

Spatial patterns of maize harvest date are rather well reproduced by the model (Figure 3(c, e, f)). According to both observations and simulations, large regions of North America, Eastern Europe, and Russia show similar values (no differences in Fig.2(f)), indicating convergence of maize harvest dates in mid-temperature areas. In these areas the gradients in GPs are therefore a result of gradients sowing dates. Similarly, good agreement with the observation is found in South America, with homogeneous harvest time and GP found over large parts of the continent.

The model systematically overestimates the end of the growing period in Central Africa and Eastern China. Differences between the computed and observed harvest date are found e.g. in Mexico, around the Mediterranean Sea, and in South-Eastern China. In these areas, MIRCA2000 reports homogeneous values, while the model simulates gradients. From Figure 3(f) it can be seen that there is a shift from -1 to +1 months difference across these gradients. For example, harvest in Spain goes from August-September to October progressing from south to north. In these areas, the observations report harvest homogeneously for September.

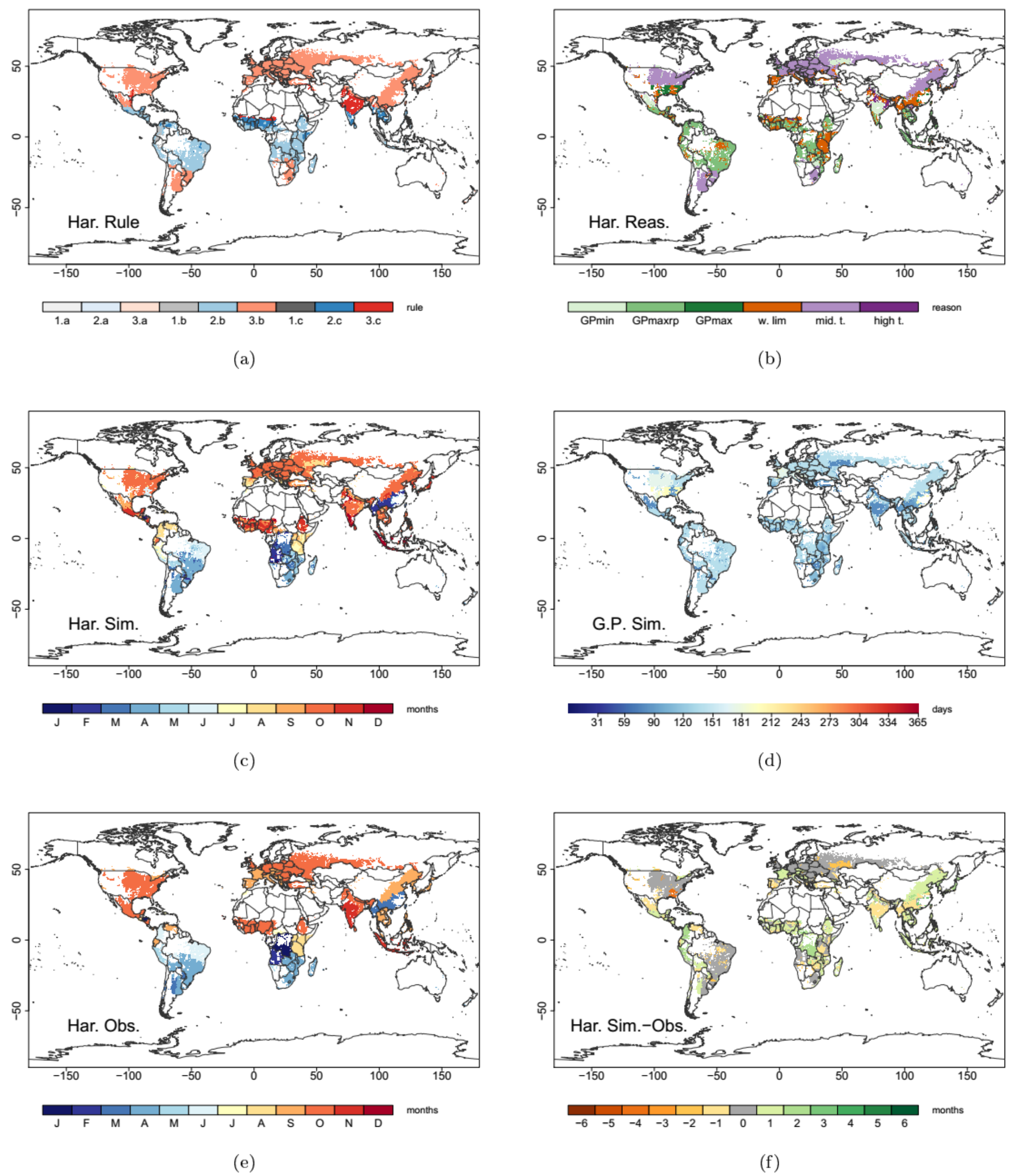

Figure 3: Maize, (a) agro-climatic zones of cultivation and corresponding rule applied for computing the maturity date; (b) maturity date reason, or the factor causing the end of the growing period; (c); computed harvest month; (d) length (days) of the computed total growing period (GP); (e) observed harvest month from MIRCA2000; (f) difference between computed and observed harvest month. White color indicates pixels with less than 0.001\% maize cultivated area. 1.a-3.c indicate the

different agro-climatic zones and the corresponding harvest date rule. GPmin is earliest-maturing cultivar; GPmaxrp is longest grain-fill cultivar; GPmax is latest-maturing cultivar; w.lim is water limitations; mid. t. is mid-temperature limitations; hight t. is high-temperature limitations.

Compared to maize, the other five crops have growing seasons more likely affected by non-optimal temperatures. In particular, the high temperature rules (1.c, 2.c, 3.c) apply to the largest fraction of the current cultivated area of rice, sorghum and soybean (Figure E1, E3 in appendix), which require cultivars with a longer growing period to avoid the high-temperature during the reproductive phase.

Patterns of soybean GP are relatively similar to those of maize, while generally spring-wheat and sorghum show shorter GPs. For winter-wheat GPs are mostly calculated as very long (7 to 11 month), with increasing lengths in colder regions (central-Europe and Russia). Sub-Tropical regions show quite uniform GP durations and similar among different crops (e.g. maize, sorghum, rice in Sub-Saharan Africa). Though in India, GP differs between crops because the maturity date is triggered by different reasons. Similarly to maize the spatial patterns of harvest dates are well reproduced by the model for all crops. Winter-wheat and soybean show gradients of harvest dates, due to gradients in the driving climatic factors (e.g. temperature patterns in the United States), leading to differences to the observations, which report uniform values within geographical units.

3.3. Full simulation of the cropping periods

Results for both simulated sowing and harvest and their difference to MIRCA2000 are shown in Appendix G. Simulated cropping periods are displayed for the entire global land, therefore also in regions where crops are not currently grown. Simulations and observations show similar degrees of agreement for both sowing and harvest dates, with coinciding spots of largest differences e.g. south-eastern China, southern Brazil, Tanzania for maize (Appendix G). The duration of the total GP shows good agreement with the observed one, even in the areas where sowing and/or harvest dates deviate from observations. Indeed, the sign of the simulated to observed difference is in most cases the same although there are some exceptions. Winter-wheat in the USA shows at the same time delayed sowing and anticipated harvest, resulting in an overall shorter GP with respect to MIRCA2000. Soybean in south-eastern China results in longer GP, due to an earlier sowing and a delayed harvest.

4. Discussion

We show that average maturity (and harvest) dates can be estimated from crop-specific plant physiological parameters and climatic conditions for the majority of currently cropped areas . For the largest part of the global cultivated land the model results are in agreement with both MIRCA2000 (dataset used for model calibration) and SAGE (independent dataset). The mean absolute error (MAE) is close to or lower than about 1 month for all the considered crops. On a local scale or within a single year, a difference of a month in the maturity date of a crop could make a substantial difference e.g. for the crop productivity. However, such an error value is not large when considering the global scale of this study. Similar errors were obtained for sowing dates (Waha et al., 2012) and growing periods (van Bussel et al., 2015; Mathison et al., 2018). Differences can be explained partly by limitations in the modelling approach, and partly by shortcomings in the datasets used for comparison. MIRCA2000 reports dates with a monthly resolution. This means that when using this observation-based dataset as input to models with a daily time step assumptions must be made for converting months to days. This necessarily introduces an uncertainty of about a month in the observations themselves. On the other hand, SAGE has a daily resolution. Despites, its use is also subject to uncertainty due to low resolved spatial patterns (e.g. uniform country values) and to the large reported ranges around sowing and harvest dates. These shortcomings do not leave much room for improving the accuracy in our model evaluation. In addition, the authors of the MIRCA2000 dataset recommend caution in using such cropping dates "in areas where local biophysical constraints differ considerably from average constrains within the calendar unit" (Portmann et al., 2010). We find that where the data are homogeneous over large areas, the model can simulate spatial gradients distributed around the average maturity date. In such cases, the simulated maturity dates seem to be more realistic than the observed ones.

The two previously proposed approaches for the estimation of crop maturity or harvest dates that we could find in the literature are more empirically based, as they directly derive rules by crop calendar observations and climate data. The method from van Bussel et al. (2015), computes location-specific cultivar parameters (thermal units requirements, vernalization and photoperiod) with linear-regression models, and from these derives harvest dates. Mathison et al. (2018) models the rice–wheat rotation calendar in South Asia based on the Asian Summer Monsoon. They derive the sowing and harvest date rules by simply computing the difference between onset/cessation of the monsoon and the observed sowing/harvest dates, and determining the weighted area averages from these to derive the rule. With a similar performance in terms of estimation error, our approach has the advantage of being more process-based which allows for better understanding of underlying mechanisms of cropping periods selection and for more explicit assumptions on future crop varieties' choice scenarios (e.g. different crop sensitivities to temperature, or crop phenological phase durations).

The results show that a single set of rules (with crop-specific parameters) is valid for simulating the average current growing periods of any of the grain crops. Even though the model represents a very complex decision making process in a simplified way, its ability to reproduce global cropping calendar variability and patterns suggests that a few climatic variables and crop physiological limits can explain a large portion of the recent cropping period patterns. This endorses the idea that agricultural practices have been adapting to the climatic conditions experienced by farmers (Olesen et al., 2012). Specifically, it shows that farmers tend to grow the crops under the best available conditions for maximizing crop productivity. In particular, the timing of the reproductive phase seems to be a general criterion for selecting grain crops cultivars. In environments characterized by temperature seasonality, where the first phases of the crop cycles are subject to cooler temperatures (e.g. winter-wheat), it seems a common practice to extend the growing period, and therefore prolong the vegetative development (Appendix F, panels d), to let the reproductive phase occurring within the warmest season. However, stressful temperatures or water-scarce seasons can require the use of shorter or longer maturing cultivars. In line with previous findings (Egli, 2011; Hay & Porter, 2006; Parent et al., 2018), we assume a much larger flexibility of the vegetative phase length, as compared to a more stable reproductive phase. However, it has been shown that crop breeding has in some cases targeted earlier flowering and extended the reproductive phases (Glotter & Elliott, 2016). As we explicitly parametrize this in our model, it is possible to account for such genetic improvement in future studies.

On farms, when selecting for cultivars and cropping periods, farmers may take into account several factors (e.g. soil conditions, yield potentials, pests and diseases, consumer preferences) that are not explicitly considered in our model. In consequence, as for the simulation of sowing dates (Waha et al., 2012), the model performs very well in regions with clearly climate-defined growing periods, as temperate zones, or sub-tropical regions with strong precipitation seasonality. It results in larger deviations in regions with long suitable growing seasons that allow for more flexibility in timing of agricultural operations. Moreover, the model does not consider multiple cropping systems or crop rotations, but addresses single-crop systems only. The cultivation of different crops in a sequence can nevertheless constrain the growing periods of each single crop. In temperate and continental regions, the rotations typically include both winter and summer crop types (Kollas et al. 2015). In such cases harvest and sowing of two consecutive crops are in rapid succession, leading to e.g. delayed sowing of the winter crop. However, it has been shown that there is convergence of anthesis and maturity dates of winter crops, that results in similar harvest times for crops sown several weeks apart (Hay & Porter, 2006). In sub-tropical regions, long and favorable growing seasons often allow for sequential cropping systems, where two crops are grown in sequence within a single growing season. These systems can be more productive than the cultivation of the longest-growing cultivar of a single crop (Waha et al., 2013). In the model, we account for a maximum growing period length, beyond which there is no further yield benefit (GPmaxrp). For future model applications, this feature could allow for using the remaining suitable growing period for a second crop cycle in the same year. We apply a crop-specific parametrization, even though differences exist not only among species, but also among cultivars or subspecies, such as *Indica* or *Japonica* rice (Sánchez et al., 2014). Knowledge on cultivar-specific characteristics would improve the model applicability, although to evaluate the performances of such parametrization, one would require spatially explicit datasets on cultivars, as well as on their cropping periods, which may be difficult to retrieve even at a regional scale.

The model does not account either for soil water holding capacity or any water-harvesting, or soil moisture conservation practices (Jägermeyr et al., 2016), which exist even in rainfed systems. These could be the reason for the underestimated GPs (harvest dates are simulated earlier than observations), e.g. maize in India and Mexico. Similarly, the large fraction of underestimated rice harvest dates (e.g. -3 months difference for rice panel Figure 2, Southeast-Asia and Colombia, Appendix F) may derive from different assumptions on water management in the model and MIRCA2000. This dataset assigns standard GP lengths to three classes of rainfed rice cultivation systems (7 to 8 months to upland-; 7 months to deep-water-; 4 months to paddy-rice systems). This suggests that the maximum GP that we assume in these areas is not parameterized well for rice and that a higher threshold (GP_{maxrp}) could lead to a substantial model improvement in these areas. Although such extended observed GPs might coincide with deep-water rice (flooded) (Khush, 1984), this practice is not considered in the model. Moreover, upland rice can have shorter GP (Khush, 1984) than those assumed by MIRCA2000. In the same areas, both MIRCA2000 and SAGE report secondary growing periods of rice with much shorter (3 to 4 months) durations (not shown here), which are closer to our results. To include explicit simulation of the soil water content into our modelling approach would drastically increase its complexity, and the number of simulated processes and assumptions. This would in fact require the use of a global crop-hydrological model (e.g. Schaphoff et al., 2017) with dynamic simulation of soil-plant hydrological processes and with additional input datasets on soil types, weather variables, and water management. We have shown that the end of the reported growing periods coincides respectively with a declining or peaking trends of the two simple indicators based on the P to PET ratio, that we therefore consider good indicators of dryness that can be used for large parts of the simulated land area.

Our findings show that it is generally possible to compute growing periods, defined by sowing dates (Waha et al., 2012) and maturity dates (this study) from climatic parameters. To our knowledge, this is the first study that presents a methodology to directly estimate maturity dates at the global scale, without relying on GDD computation. Note that the model should not be used for directly estimating interannual variability in crop phenology. This method provides a dataset that can be used to parametrize crop phenology without relying on any particular phenological model. It can be used to fill data gaps or to estimate cropping periods outside the current cropland as done by Elliott et al. (2015) for the sowing dates. The combination of sowing and harvest date function also allows for embedding agricultural management decisions on the cropping periods within global crop modelling approaches, where the assumption is often that farmers do not adjust to changes in growing seasons (Rosenzweig et al., 2014). Uncertainty about future climate can be accounted for by running our algorithm with different climate datasets. Under extreme scenarios it is likely that the model would not find suitable growing periods for the crops. In such case, as for the currently unsuitable regions, the algorithm would choose the shortest maturing cultivar. Moreover, the model allows for studying changes in crop sensitivity to temperature or precipitation due to breeding or to technological change, as the crop physiological limits are explicitly represented. This enables to account for autonomous adaptation in crop model simulations, but comes at the price that cultivation systems in some regions (e.g. tropics) can only be presented less well for current conditions than if sowing dates were prescribed (Elliott et al., 2015; Müller et al., 2017). The implications of this need to be tested with the model-specific parameterization of crop species and will have to be considered in the interpretation of results.

5. Acknowledgments

This work is part of the MACMIT project (01LN1317A), funded by the German Ministry for Education and Research (BMBF). The authors gratefully thank Frank Wechsung, as well as the members of the LandUse and LPJmL groups at PIK for their support and helpful comments; the GGCMI project for providing access to the AgMERRA dataset; the European Regional Development Fund (ERDF), the BMBF, and the Land Brandenburg for providing resources on the high performance computer system at PIK.

6. Appendices

A. Illustration of the maturity date rule
B. Observed growing periods
C. P to PET ratio analysis
D. Sensitivity analysis
E. Aggregated model performances
F. Global maps of computed harvest dates for all crops
G. Global maps of computed sowing, harvest, total growing period for all crops
H. Algorithm (R code) to determine location-specific maturity (or harvest) dates

7. Data availability

Ncdf4 data files of computed sowing and harvest dates, corresponding to figures in Appendix G are associated to this article. All other data (model input and output), as well as the R scripts used for generating the results of this study are available from the author upon request at: sara.minoli@pik-potsdam.de.

8. References

Ainsworth, E.A. & Ort, D.R. (2010) How do we improve crop production in a warming world? *Plant Physiol*, **154**, 526-30.

Araya, A., Keesstra, S.D. & Stroosnijder, L. (2010) A new agro-climatic classification for crop suitability zoning in northern semi-arid Ethiopia. *Agricultural and Forest Meteorology*, **150**, 1057-1064.

Archontoulis, S. V., Miguez, F. E., & Moore, K. J. (2014). A methodology and an optimization tool to calibrate phenology of short-day species included in the APSIM PLANT model: Application to soybean. Environmental Modelling and Software, 62, 465–477. http://doi.org/10.1016/j.envsoft.2014.04.009

Asseng, S., Zhu, Y., Wang, E. & Zhang, W. (2015) Crop modeling for climate change impact and adaptation. 505-546.

Bodner, G., Nakhforoosh, A. & Kaul, H.-P. (2015) Management of crop water under drought: a review. *Agronomy for Sustainable Development*, **35**, 401-442.

Bondeau, A., Smith, P.C., Zaehle, S., Schaphoff, S., Lucht, W., Cramer, W., Gerten, D., Lotze-Campen, H., MÜLler, C., Reichstein, M. & Smith, B. (2007) Modelling the role of agriculture for the 20th century global terrestrial carbon balance. *Global Change Biology*, **13**, 679-706.

Challinor, A.J., Koehler, A.K., Ramirez-Villegas, J., Whitfield, S. & Das, B. (2016) Current warming will reduce yields unless maize breeding and seed systems adapt immediately. *Nature Climate Change*, **6**, 954-958.

Clerget, B., Dingkuhn, M., Goze, E., Rattunde, H.F. & Ney, B. (2008) Variability of phyllochron, plastochron and rate of increase in height in photoperiod-sensitive sorghum varieties. *Ann Bot*, **101**, 579-94.

Craufurd, P. & Qi, A. (2001) Photothermal adaptation of sorghum (Sorghum bicolour) in Nigeria. *Agricultural and Forest Meteorology*, **108**, 199-211.

Craufurd, P.Q. & Wheeler, T.R. (2009) Climate change and the flowering time of annual crops. *J Exp Bot*, **60**, 2529-39.

Deryng, D., Sacks, W.J., Barford, C.C. & Ramankutty, N. (2011) Simulating the effects of climate and agricultural management practices on global crop yield. *Global Biogeochemical Cycles*, **25**, n/a-n/a.

Dobor, L., Barcza, Z., Hlásny, T., Árendás, T., Spitkó, T. & Fodor, N. (2016) Crop planting date matters: Estimation methods and effect on future yields. *Agricultural and Forest Meteorology*, **223**, 103-115.

Drewniak, B., Song, J., Prell, J., Kotamarthi, V.R. & Jacob, R. (2013) Modeling agriculture in the Community Land Model. *Geoscientific Model Development*, **6**, 495-515.

Egli, D.B. (2011) Time and the productivity of agronomic crops and cropping systems. *Agronomy journal*, **103**, 743-750.

Elliott, J., Müller, C., Deryng, D., Chryssanthacopoulos, J., Boote, K.J., Büchner, M., Foster, I., Glotter, M., Heinke, J., Iizumi, T., Izaurralde, R.C., Mueller, N.D., Ray, D.K., Rosenzweig, C., Ruane, A.C. & Sheffield, J. (2015) The Global Gridded Crop Model Intercomparison: data and modeling protocols for Phase 1 (v1.0). *Geoscientific Model Development*, **8**, 261-277.

Farooq, M., Bramley, H., Palta, J.A. & Siddique, K.H.M. (2011) Heat Stress in Wheat during Reproductive and Grain-Filling Phases. *Critical Reviews in Plant Sciences*, **30**, 491-507.

Gerten, D., Schaphoff, S., Haberlandt, U., Lucht, W. & Sitch, S. (2004) Terrestrial vegetation and water balance—hydrological evaluation of a dynamic global vegetation model. *Journal of Hydrology*, **286**, 249-270.

Glotter, M., & Elliott, J. (2016). Simulating US agriculture in a modern Dust Bowl drought. *Nature plants*, 3, 16193.

Hay, R. K., & Porter, J. R. (2006). The physiology of crop yield. Blackwell Publishing.Hatfield, J.L., Boote, K. J., Kimball, B. A., Ziska, L. H., Izaurralde, R. C., Ort, D., ... & Wolfe, D. (2011) Climate Impacts on Agriculture: Implications for Crop Production. *Agronomy journal*, **103**, 351-370.

IPCC, 2013: Climate Change 2013: The Physical Science Basis. Contribution of Working Group I to the Fifth Assessment Report of the Intergovernmental Panel on Climate Change [Stocker, T.F., D. Qin, G.-K. Plattner, M. Tignor, S.K. Allen, J. Boschung, A. Nauels, Y. Xia, V. Bex and P.M. Midgley (eds.)]. Cambridge University Press, Cambridge, United Kingdom and New York, NY, USA, 1535 pp

Jachner, S., Van den Boogaart, G. & Petzoldt, T. (2007) Statistical methods for the qualitative assessment of dynamic models with time delay (R Package qualV). *Journal of Statistical Software*, **22**, 1-30.

Jägermeyr, J., & Frieler, K. (2018). Spatial variations in crop growing seasons pivotal to reproduce global fluctuations in maize and wheat yields. *Science advances*, **4**, eaat4517.

Jägermeyr, J., Gerten, D., Schaphoff, S., Heinke, J., Lucht, W. & Rockström, J. (2016) Integrated crop water management might sustainably halve the global food gap. *Environmental Research Letters*, **11**, 025002.

Khush, G. (1984) Terminology for rice growing environments. *Terminology for rice growing environments*, 5-10.

Koehler, A.-K., Challinor, A.J., Hawkins, E. & Asseng, S. (2013) Influences of increasing temperature on Indian wheat: quantifying limits to predictability. *Environmental Research Letters*, **8**, 034016.

Kollas, C., Kersebaum, K. C., Nendel, C., Manevski, K., Müller, C., Palosuo, T., ... & Conradt, T. (2015). Crop rotation modelling—A European model intercomparison. *European Journal of Agronomy*, 70, 98-111.

Kucharik, C.J. & Brye, K.R. (2003) Integrated BIosphere Simulator (IBIS) yield and nitrate loss predictions for Wisconsin maize receiving varied amounts of nitrogen fertilizer. *Journal of environmental quality*, **32**, 247-268.

Lawn, R., Summerfield, R., Ellis, R., Qi, A., Roberts, E., Chay, P., Brouwer, J., Rose, J. & Yeates, S. (1995) Towards the reliable prediction of time to flowering in six annual crops. VI. Applications in crop improvement. *Experimental Agriculture*, **31**, 89-108.

Lindeskog, M., Arneth, A., Bondeau, A., Waha, K., Seaquist, J., Olin, S. & Smith, B. (2013) Implications of accounting for land use in simulations of ecosystem carbon cycling in Africa. *Earth System Dynamics*, **4**, 385-407.

Macholdt, J. & Honermeier, B. (2016) Impact of Climate Change on Cultivar Choice: Adaptation Strategies of Farmers and Advisors in German Cereal Production. *Agronomy*, **6**, 40.

Makowski, D., Nesme, T., Papy, F. & Doré, T. (2014) Global agronomy, a new field of research. A review. *Agronomy for Sustainable Development*, **34**, 293-307.

Mathison, C., Deva, C., Falloon, P., & Challinor, A. J. (2018). Estimating sowing and harvest dates based on the Asian summer monsoon. Earth System Dynamics, 9(2), 563–592.Meier, U. (1997) *Growth stages of mono-and dicotyledonous plants*. Blackwell Wissenschafts-Verlag, Berlin, Wien.

Müller, C., Elliott, J., Chryssanthacopoulos, J., Arneth, A., Balkovic, J., Ciais, P., Deryng, D., Folberth, C., Glotter, M., Hoek, S., Iizumi, T., Izaurralde, R.C., Jones, C., Khabarov, N., Lawrence, P., Liu, W., Olin, S., Pugh, T.A.M., Ray, D.K., Reddy, A., Rosenzweig, C., Ruane, A.C., Sakurai, G., Schmid, E., Skalsky, R., Song, C.X., Wang, X., de Wit, A. & Yang, H. (2017) Global gridded crop model evaluation: benchmarking, skills, deficiencies and implications. *Geoscientific Model Development*, **10**, 1403-1422.

Olesen, J.E., Borgesen, C.D., Elsgaard, L., Palosuo, T., Rotter, R.P., Skjelvag, A.O., Peltonen-Sainio, P., Borjesson, T., Trnka, M., Ewert, F., Siebert, S., Brisson, N., Eitzinger, J., van Asselt, E.D., Oberforster, M. & van der Fels-Klerx, H.J. (2012) Changes in time of sowing, flowering and maturity of cereals in Europe under climate change. *Food Addit Contam Part A Chem Anal Control Expo Risk Assess*, **29**, 1527-42.

Parent, B., Leclere, M., Lacube, S., Semenov, M. A., Welcker, C., Martre, P., & Tardieu, F. (2018). Maize yields over Europe may increase in spite of climate change, with an appropriate use of the genetic variability of flowering time. *Proceedings of the National Academy of Sciences*, 115(42), 10642-10647.

Parent, B. & Tardieu, F. (2012) Temperature responses of developmental processes have not been affected by breeding in different ecological areas for 17 crop species. *New Phytol*, **194**, 760-74.

Peltonen-Sainio, P., Rajala, A., Känkänen, H. & Hakala, K. (2015) Chapter 4 - Improving farming systems in northern

Europe A2 - Sadras, Victor O. *Crop Physiology (Second Edition)* (ed. by D.F. Calderini), pp. 65-91. Academic Press, San Diego.

Porter, J.R., & Gawith, M. (1999) Temperatures and the growth and development of wheat: a review. *European Journal of Agronomy*, **10**, 23-36.

Porter, J.R. & Semenov, M.A. (2005) Crop responses to climatic variation. *Philosophical Transactions of the Royal Society B: Biological Sciences*, **360**, 2021-2035.

Porter, J.R., Xie, L., Challinor, A.J., Cochrane, K., Howden, S.M., Iqbal, M.M., Lobell, D.B. & Travasso, M.I. (2014) Chapter 7: Food security and food production systems. In. Cambridge University Press

Portmann, F.T., Siebert, S. & Döll, P. (2010) MIRCA2000-Global monthly irrigated and rainfed crop areas around the year 2000: A new high-resolution data set for agricultural and hydrological modeling. *Global Biogeochemical Cycles*, **24**, n/a-n/a.

Priestley, C.H.B., & Taylor, R. J. (1972) On the assessment of surface heat flux and evaporation using large-scale parameters. *Monthly weather review*, **100**, 81-92.

Ritchie, J.T. & Nesmith, D.S. (1991) Temperature and Crop Development. *Modeling Plant and Soil Systems*, pp. 5-29. American Society of Agronomy, Crop Science Society of America, Soil Science Society of America, Madison, WI.

Rosenzweig, C., Elliott, J., Deryng, D., Ruane, A. C., Müller, C., Arneth, A., ... & Neumann, K. (2014) Assessing agricultural risks of climate change in the 21st century in a global gridded crop model intercomparison. *Proceedings of the National Academy of Sciences*, **111**, 3268-3273.

Ruane, A.C., Goldberg, R. & Chryssanthacopoulos, J. (2015) Climate forcing datasets for agricultural modeling: Merged products for gap-filling and historical climate series estimation. *Agricultural and Forest Meteorology*, **200**, 233-248.

Rukhovich, D.I., Koroleva, P.V., Vilchevskaya, E.V., Romanenkov, V.A. & Kolesnikova, L.G. (2007) Constructing a spatially-resolved database for modelling soil organic carbon stocks of croplands in European Russia. *Regional Environmental Change*, **7**, 51-61.

Sacks, W.J., Deryng, D., Foley, J.A. & Ramankutty, N. (2010) Crop planting dates: an analysis of global patterns. *Global Ecology and Biogeography*, no-no.

Sánchez, B., Rasmussen, A. & Porter, J.R. (2014) Temperatures and the growth and development of maize and rice: a review. *Glob Chang Biol*, **20**, 408-17.

Schaphoff, S., Von Bloh, W., Rammig, A., Thonicke, K., Biemans, H., Forkel, M., ... & Langerwisch, F. (2018). LPJmL4–a dynamic global vegetation model with managed land–Part 1: Model description. *Geoscientific Model Development*, 11, 1343-1375.

Sedgley, R.H. (1991) An appraisal of the Donald ideotype after 21 years. . *Field Crops Research*, **26**, 93-112.

Singh, R.P., Prasad, P. V., & Reddy, K. R. (2013) Impacts of changing climate and climate variability on seed production and seed industry. *Advances in Agronomy*, **118**, 49-110.

Slafer, G.A., Kantolic, A., Appendino, M., Tranquilli, G., Savin, R., Miralles, D., Sadras, V. & Calderini, D. (2015) Genetic and environmental effects on crop development determining adaptation and yield. *Crop Physiology: Applications for Genetic Improvement and Agronomy*, pp. 285-319. Academic Press San Diego.

Team, R.C. (2015) *R: A language and environment for statistical computing.*

Thornthwaite, C.W. (1948) An Approach toward a Rational Classification of Climate. *Geographical Review*, **38**, 55-94.

Tomich, T. P., Brodt, S., Ferris, H., Galt, R., Horwath, W. R., Kebreab, E., … Yang, L. (2011). Agroecology: A Review from a Global-Change Perspective. Annual Review of Environment and Resources, 36(1), 193–222. http://doi.org/10.1146/annurev-environ-012110-121302

van Bussel, L.G.J., Stehfest, E., Siebert, S., Müller, C. & Ewert, F. (2015) Simulation of the phenological development of wheat and maize at the global scale. *Global Ecology and Biogeography*, **24**, 1018-1029.

van Wart, J., van Bussel, L.G.J., Wolf, J., Licker, R., Grassini, P., Nelson, A., Boogaard, H., Gerber, J., Mueller, N.D., Claessens, L., van Ittersum, M.K. & Cassman, K.G. (2013) Use of agro-climatic zones to upscale simulated crop yield potential. *Field Crops Research*, **143**, 44-55.

Waha, K., van Bussel, L.G.J., Müller, C. & Bondeau, A. (2012) Climate-driven simulation of global crop sowing dates. *Global Ecology and Biogeography*, **21**, 247-259.

Waha, K., Müller, C., Bondeau, A., Dietrich, J.P., Kurukulasuriya, P., Heinke, J. & Lotze-Campen, H. (2013) Adaptation to climate change through the choice of cropping system and sowing date in sub-Saharan Africa. *Global Environmental Change*, **23**, 130-143.

Wang, E., Martre, P., Zhao, Z., Ewert, F., Maiorano, A., Rötter, R. P., … Asseng, S. (2017). The uncertainty of crop yield projections is reduced by improved temperature response functions. Nature Plants, 3(July), 1–11. http://doi.org/10.1038/nplants.2017.102

Wassmann, R., Jagadish, S.V.K., Heuer, S., Ismail, A., Redona, E., Serraj, R., Singh, R.K., Howell, G., Pathak, H. & Sumfleth, K. (2009) Chapter 2 Climate Change Affecting Rice Production. **101**, 59-122.